

An investigation of local and regional sources of fine particulate matter in Ostrava, the Czech Republic

Teri Vossler¹, Libor Černíkovský², Jiří Novák², Helena Plachá², Blanka Krejčí², Irina Nikolová², Eva Chalupníčková², Ronald Williams¹

¹U.S. Environmental Protection Agency, Office of Research and Development, Research Triangle Park,
North Carolina, USA

²Czech Hydrometeorological Institute, Prague, Czech Republic

Corresponding Author:

Teri Vossler

U.S. Environmental Protection Agency

Mail Drop E205-03

Research Triangle Park, NC, 27711

Phone: (919)-541-3157; FAX: (919)-541-0960

CONNER.TERI@EPA.GOV

Disclaimer

The United States Environmental Protection Agency through its Office of Research and Development collaborated with the Czech Hydrometeorological Institute in the research described here. It has been subjected to Agency review and approved for publication.

Abstract

Despite efforts to reduce air pollutants, particularly in the coal power plant and industrial sectors, the Ostrava region of the Czech Republic continues to experience episodes of high pollutant concentrations, especially during the fall and winter seasons. A short-term pilot investigation was conducted to improve understanding of air pollution sources that may be impacting the Ostrava air quality. Fine particulate matter (PM_{2.5}) samples were collected in consecutive 12-hour day and night increments during spring and fall 2012 sampling campaigns. Sampling sites were strategically located to evaluate conditions in close proximity of a large steel works industrial complex, as well as away from direct influence of the industrial complex. These samples were analyzed for metals, organic and elemental (black) carbon, and selected polycyclic aromatic hydrocarbons (PAHs). The PM_{2.5} samples were supplemented with continuous monitoring of gases and meteorological parameters. On average, the fine particulate matter mass concentrations during the fall were more than twice the average concentrations during the spring at each sampling site. Likewise, concentrations for most individual species were higher in the fall than in the spring. However, concentrations of crustal elements were higher in the spring than in the fall. Diurnal differences in fine mass concentrations were less pronounced than seasonal differences, with concentrations slightly higher at night at each site. The summed PAH concentrations increased with proximity to the industrial complex. Overall, the results indicate a source or group of sources to the northeast of all sampling sites that contributes significantly to the fine particle mass concentrations in the fall, and competes with contributions from the local industrial complex in the spring. The data presented here provide a qualitative overview of the results and form a solid foundation for the application of source apportionment models to be presented elsewhere.

Keywords

fine particulate matter

Czech Republic

steel manufacturing

home heating

black carbon

1. Introduction

Prior to 1990, the region currently known as the Czech Republic reported among the highest levels of air pollution in Europe, mostly in the form of particulate matter and SO₂ from industry, mining, and power generation (Moldan and Schnoor, 1992). Since the Velvet Revolution of 1989, the Czech Republic has invested heavily in the reduction of air pollutants, particularly in the coal power plant and industrial sectors. However, the 2000s saw an increase in traffic and industries, leading to deterioration in air quality (EEA, 2010; Czech Statistical Office, 2013; Ministry of the Environment of the Czech Republic, 2013; EEA, 2014). Though natural gas is the most commonly used heating fuel, an increase in energy prices has forced some households to use cheaper fuels, such as high-sulfur coal, wood, and municipal waste to heat their homes (Ministry of the Environment of the Czech Republic, 2013).

The Moravian-Silesian region on the northeast border has particular challenges due to its ongoing industrial presence, and remains the air pollution hot-spot of the Czech Republic, despite recent reductions in steel production and mining operations (EEA, 2014). The region is bordered by the Beskydy mountain range to the southeast and the Jeseníky mountain range to the northwest, forming part of a valley known as the Moravian Gate. The valley extends from the southwest to the northeast and into the Silesian region of Poland, which also has among the highest levels of air pollution in Europe (EEA, 2014). Air flow typically follows the length of the valley, predominantly from the southwest.

Ostrava, the capital of the region and the third largest city in the Czech Republic with a population of over 300,000, is located within this valley. Ostrava's geographical setting, combined with weather-related temperature inversions and the ongoing heavy industrialization of the region, leads to episodes of high pollutant concentrations, especially during the fall and winter seasons. Ostrava is home to the largest steel works facility in the Czech Republic. The principal production facilities of this industrial complex include coke oven batteries, sinter plants, blast furnaces, open hearth tandem furnaces,

continuous casters, rolling mills, and a power plant. The coke oven batteries are of particular concern due to their emissions of polycyclic aromatic hydrocarbons (PAH) including benzo(a)pyrene and benzo(a)anthracene, which have been shown to cause cancer in laboratory animals, and have been identified as probable human carcinogens (ATSDR, 1995). Concentrations of particulate matter and benzo(a)pyrene measured at a permanent measuring station (Radvanice) downwind from the industrial complex (based on prevailing winds) are higher than at other locations in Ostrava. Other major sources of air pollutants in the region that may impact air quality include coal-fired power plants, which provide power-generation for domestic and industrial use; home heating by a variety of fuel types including natural gas, coal, and wood; and transportation, primarily cars and buses fueled by standard gasoline and diesel fuel (Ministry of the Environment of the Czech Republic, 2013; EEA, 2014).

In response to concerns about on-going pollution issues, and in particular about harmful pollutants emitted by the industrial complex, the Czech Hydrometeorological Institute (CHMI) requested assistance from the US EPA's Office of Research and Development (ORD) in designing and conducting a short-term pilot investigation to improve understanding of air pollution sources that may be impacting the Ostrava air quality.

The U.S. EPA previously collaborated with Czech Republic to study its air quality problems in the early to mid-1990s. The first study was conducted over a period of several years in the city of Teplice (Stevens et al., 1996). A second short-term air quality monitoring and receptor modeling study was conducted in 1995 in the city of Ostrava (Willis et al., 1997), the site of the current collaboration. In addition, personal exposure levels of carcinogenic PAHs were measured in a select Ostrava cohort (Williams et al., 1997). In these earlier studies, ambient and source samples were collected for application in the Chemical Mass Balance (CMB) receptor model. In Teplice, notable results were that 1) winter stagnation episodes were dominated by emissions from power plants and coal-fueled home heating, 2) home

heating was a significant source of PAHs in the winter, and 3) residential space heating was a major source of fine particulate matter (Pinto et al., 1998). In Ostrava, poor model fits were obtained for samples associated with NE winds, leading to the conclusion that there was a missing source – possibly home heating with low-quality fuels such as coal or wood, since no profiles were obtained for this emission source. In addition, it was recommended that future studies reduce uncertainties in the source profiles, that source signatures be acquired for local home heating and resuspended street dust, and that an improved motor vehicle signature should be developed. (Willis et al., 1997) However, these recommendations are based on the assumption of CMB as the receptor model of choice.

In the current study, Ostrava is re-visited. As a short-term pilot effort, this study is not designed to answer all questions associated with Ostrava air quality. Rather, its intent is to provide Czech air quality risk assessors with insight into the probable industrial and regional sources impacting citizens living in Ostrava. Some of the source profile pitfalls of previous studies in the area are avoided with the planned application of more advanced multivariate receptor models as well as with some improved sampling and modeling approaches. Here we report on the general data findings with the objective not to provide a quantitative source allocation but to present qualitative results in a manner that shows the general trends. The specific source apportionment work will be reported elsewhere (Vossler et al, in preparation).

2. Methods

2.1. Sampling and Monitoring

Field sample collection and monitoring was conducted at three sampling sites over two seven-week periods in 2012. The intention was to sample during the period of the year influenced by emissions from local heating, and for comparison, during the period without this influence. However, it was necessary to minimize multi-day smog situations characterized by a stable atmospheric conditions and low wind speed/calm/variable wind directions, which occur most frequently in the December through February time frame. The air is more homogenous during such situations, confounding the investigation of directional dependence of concentrations and reducing the variability of concentrations that is needed for source apportionment. Therefore, we selected mid-October through early-December as a period likely to have regular home heating but also less prone to persistent stagnation. For the meteorologically opposite condition, we selected mid-May through early July, which does cover part of the calendar summer and has mild conditions and minimal heating. Specifically, sampling was conducted during late spring/early summer (5/14/2012 through 7/1/2012) and during late fall (10/17/2012 through 12/6/2012) to capture emissions from two distinct seasons. These will be referred to simply as “spring” and “fall” samples.

Samples were collected at three sampling sites, as shown in Figure 1. Two of the sites were strategically located to evaluate conditions upwind and downwind of the steel-making industrial complex based on prevailing southwest winds as evaluated over a 10-year period (see Figure S1 in supporting material). Radvanice is a suburban industrial site downwind of prevailing winds from the industrial complex; Vratimov is a residential area site upwind of prevailing winds from the industrial complex. The third sampling site – Poruba - was selected as a representative of the Ostrava area without immediate influence of industrial complex or other specific point sources, and was located established regulatory

monitoring sites with existing infrastructure. Each monitoring site was located in an open area away from near road influences.

[Figure 1]

Details of the sampling and monitoring plan is presented in Table S1 (see the supporting material).

Fine particulate matter (PM_{2.5}) samples were collected in consecutive 12-hour daytime and night-time increments at each sampling site to assess diurnal patterns in the data. Samples for gravimetric mass measurement and elemental analyses were collected on 47 mm Teflon filters with the reference samplers Leckel SEQ47/50 Sequential Gravimetric Sampler (Berlin, Germany). Samples for PAH and OC/EC analyses were collected on 47 mm quartz filters with the Thermo ESM Anderson FH-95 instrument outfitted with a PM_{2.5} sampling head (ESM Andersen Instruments GmbH, Erlangen, Germany), plus a 50x100 mm polyurethane foam (PUF) to collect the gas-phase component of the PAHs. Samples for analysis of semi-volatile organic compounds (SVOCs) in addition to the PAHs were collected on 47 mm Teflon filters with the Leckel Small Filter Device MVS6 (Berlin, Germany). The latter samples are currently being stored and no SVOC data from these filters will be reported here. Approximately 100 fine particle filters per filter type were collected each sampling site and season, which is the minimum required for planned source apportionment modeling. Field blank filters were deployed about once per week at each sampler. Collocated filters were collected for two weeks at the Radvanice sampling site.

Meteorological parameters were measured continuously at the permanent meteorological stations located through the region, including one at the Poruba sampling site. In addition, continuous meteorological measurements including wind speed and direction were operated at the Vratimov and Radvanice sites.

The particulate matter samples were supplemented with continuous SO₂ monitoring at all three sites, and PM₁₀ and additional pollutant gas monitoring (O₃, NO, NO₂, NO_x, CO, benzene) at the Radvanice and Vratimov sites. Monitoring was conducted using EU reference methods (European Parliament, Council of the European Union, 2008).

2.2. Particulate Matter Characterization

The principal focus of the study is on the composition of the fine particulate matter, to be used in source apportionment modeling to evaluate relative source impacts on the air quality in Ostrava. Specifics of the analytical instrumentation can be found in Table S1 (see the supporting material).

Gravimetric Mass. The CHMI performed gravimetric measurements on the PM_{2.5} Teflon filter samples. Following validation of these measurements, CHMI sent the filters to the U.S. EPA for additional laboratory analyses, data evaluation, and source apportionment.

Black Carbon. EPA analyzed the PM_{2.5} Teflon filter samples for black carbon (BC) via a non-destructive dual-wavelength optical transmission method (Hansen, 2005). The instrument used in this study operates at two different wavelengths: BC is measured with the infrared (880nm) source, while a parameter referred to simply as UV-PM is measured with the ultraviolet (370 nm) source. The latter is not a real physical parameter but represents UV-absorbing material at a black carbon mass equivalence. The light attenuation measurements are based on the comparison of light absorbed by the sample filter with light absorbed by a blank reference filter. See supporting material for details of these computations and uncertainty estimates (Text S1), including Teflon filter deposit area estimates (Text S2).

Elements via Energy-Dispersive X-Ray Fluorescence. EPA subsequently measured the elemental composition of the Teflon filter samples using energy-dispersive x-ray fluorescence (EDXRF). Analyses were accomplished in 14 separate analysis runs, including duplicate analyses. The procedures followed for the analysis and data processing and the science behind those procedures are described in detail elsewhere (Kellogg, 2007).

The processing of the EDXRF analyses produces an uncertainty for every reported elemental concentration for every sample, based on propagation of uncertainties from all sources. Furthermore, all concentration values and their uncertainties produced by the least-squares process are reported, whether above or below detection levels, since they are accompanied by realistic uncertainties specific to that concentration.

Elemental and Organic Carbon. The CHMI analyzed a 1x1.5 cm piece of each quartz filter sample for elemental carbon (EC) and organic carbon (OC) via NIOSH method 5040 (NIOSH, 2003). Extended uncertainty estimates of 17% for OC and 37% for EC were applied to each sample. The extended uncertainty, also known as the method uncertainty, combines uncertainties from sampling, processing and analysis.

Polycyclic Aromatic Hydrocarbons. The CHMI analyzed the remainder of the quartz filter and the PUF (50x100 mm) for 14 polycyclic aromatic hydrocarbon (PAH) compounds via gas chromatography-mass spectrometry (GC-MS) following established methods (European Parliament, Council of the European Union, 2008). Details of the analytical procedure are described in the supporting material (Text S3). Concentrations of the combined gas (PUF) and particle (quartz filter) phases were provided for each PAH species along with species-specific error fractions and quantifiable limits (QL). Details of uncertainty

estimates for measured and replacement concentrations for species reported as <QL are described in the supporting material (Text S4).

3. Results and Discussion

Data were evaluated using seasonal and diurnal stratifications, site comparisons, time series analyses, wind sector analyses, and statistical analyses using Excel 2013 with the Analysis ToolPak Add-In. These methods provided a qualitative assessment of the possible sources and revealed outliers that should be omitted in further analyses and source apportionment modeling. Preliminary results were presented at the 2013 European Aerosol Conference in Prague, Czech Republic (Černíkovský et al., Sept. 2013).

3.1. Fine Particle Mass and Composition

Table 1 shows the average, standard deviation, and maximum value of fine mass and selected species concentrations, stratified by site and season. Elemental species with an average signal to noise of at least two in at least one reporting category (e.g., site and season) are included in the data summaries and subsequent analyses. In addition, certain species are included because of their value as a tracer for a major particulate matter source category. Thus, As and Se are included in the table based on their value as a tracer for coal combustion. Samples with any one species having an extreme concentration value (outlier) were excluded from the statistics. The criterion for exclusion was that the outlier value be twice the next highest concentration of that species. Total mass for OC was estimated using a conversion factor of 1.6 for urban aerosols as recommended by Turpin and Lim, 2001. The summed PAH concentrations are reported as Σ PAH. Benzo(a)pyrene (BaP) is also included separately because, in addition to being a probable carcinogen, it must meet established regulatory standards (European Commission, 2014).

[Table 1]

On average, the fine particulate matter mass concentrations during the fall were more than twice the average concentrations during the spring at each sampling site. Likewise, concentrations for most

individual species were higher in the fall than in the spring. However, concentrations of crustal elements Si and Ti were higher in the spring than in the fall. The concentration of crustal-generated species may be driven by field, lawn, and garden activities that are more likely in the spring and summer.

Inter-site differences in fine mass concentrations within each season were less pronounced than seasonal differences, with average concentrations highest at the Radvanice site (49.1 $\mu\text{g}/\text{m}^3$ fall, 17.2 $\mu\text{g}/\text{m}^3$ spring) and lowest at the Poruba site (35.6 $\mu\text{g}/\text{m}^3$ fall, 15.1 $\mu\text{g}/\text{m}^3$ spring). Average concentrations of most individual species were higher at the Radvanice site than at the other sites, and the concentration disparity was more pronounced in the fall than in the spring. Average concentrations of metals (esp. Mn, Fe, Zn, and Pb), Cl, and K at the Radvanice site were more than twice the concentrations at the other sites. Furthermore, time series plots of selected species at the Radvanice site (see Figure S2 in the supporting material) show concentrations of metals tracked together over time, indicating a common source – likely the industrial complex. By contrast, sulfur and carbonaceous were less variable over time and did not show the same temporal pattern as the metals at the Radvanice site, suggesting an additional source of these species.

Table 2 shows the average, standard deviation, and maximum value of fine mass and selected species concentrations, stratified by sampling time (day vs. night). Diurnal differences in fine mass concentrations were less pronounced than seasonal differences, with concentrations slightly higher at night at each site. Concentrations of carbon species, which collectively comprised more than 50% of the fine mass, were also higher at night. Likewise, Cl concentrations were higher at night, while most other elemental concentration were higher during the day. Diurnal differences in concentration suggest different source origins, such as combustion versus wind-blown particulate matter.

[Table 2]

The PAHs measured in this study have been identified as priority compounds (U.S. EPA, 1981), based on prevalence in the environment and their potential for harmful effects (ATSDR, 1995). These pollutants are mostly formed from the incomplete combustion of a variety of fuels emitted by a range of source types, including regional-scale power generation, residential heating, industrial processes, waste incineration, and mobile sources.

At the Radvanice site, the fall Σ PAH concentration (average 336 ng/m³) was significantly higher than the spring Σ PAH concentrations (average 115 ng/m³), as determined by a two-sample t-test, $p < 0.0001$. Across all sites, the Σ PAH concentrations were 3-5 times higher for the fall samples than for the spring samples. The seasonal differences can be partially explained by the atmospheric conditions in the warmer months that favor increased photolysis and dispersion of all PAHs, in contrast with conditions in the colder months that favor more frequent inversion conditions, lower mixing layer, and reduced atmospheric reaction conditions. The difference is unlikely to be associated with greater partitioning to the gas phase in the warmer months, since the reported concentrations combine the gas and particulate phases. The Σ PAH concentrations increased with proximity to the industrial complex so that the lowest concentrations were measured at the Poruba site (94 ng/m³ over both sampling seasons) and the highest concentrations were measured at Radvanice (226 ng/m³ over both sampling seasons). These inter-site differences were significant at $p < 0.0001$. Diurnal differences in PAH concentrations were less pronounced than seasonal or inter-site differences. At the Radvanice site, night concentrations were 250 ng/m³ compared with day concentrations of 202 ng/m³, a difference significant at $p < 0.05$. The Σ PAH comprised less than 1% of the fine particle mass.

3.2. Continuous Gas Monitoring Results

The continuous monitoring gas data are not included in the data summaries with the 12-hour integrated sampling particulate species data because the gas monitoring was not done consistently at all sites and seasons, and there were many more missing values among the time periods and locations that were monitored. These data are considered separately. The 1-hour average concentrations corresponding to each 12-hour integrated sampling period were averaged to produce 12-hour average concentrations that can be included in analyses with the fine particulate matter species on an equal time-averaged basis. The 12-hour concentrations were considered missing if three or more 1-hour concentrations were missing.

Select gases were compared at the Radvanice site for the spring and fall seasons (Tables S2a and S2b in the supporting material). CO was not available for the spring monitoring at Radvanice. Aside from the expected strong correlation between NO_x and NO_2 , the strongest correlations were between NO_2 and PM10 in both sampling seasons ($R=0.63$ spring; $R=0.69$ fall).

SO_2 was the only gaseous species measured at all three sampling sites. Time-series comparison of the 12-hour averaged SO_2 concentrations at the three sampling sites during the spring and fall seasons (Figure S3, supporting material) show high concentration episodes at the Radvanice site, especially in the fall monitoring season. Inter-site correlations were no greater than $R=0.27$, based on the 1-hour concentrations. The average 1-hour concentrations of SO_2 at Radvanice, Vratimov, and Poruba, respectively were $7.5 \mu\text{g}/\text{m}^3$, $6.5 \mu\text{g}/\text{m}^3$, and $3.5 \mu\text{g}/\text{m}^3$ in the spring and $17.7 \mu\text{g}/\text{m}^3$, $11.7 \mu\text{g}/\text{m}^3$, and $6.2 \mu\text{g}/\text{m}^3$ in the fall. These data suggest that SO_2 is influenced by localized activities at the industrial complex as well as seasonal factors.

3.3. Black Carbon vs Elemental Carbon

As defined by the U.S. EPA Report to Congress on Black Carbon (U.S. EPA, 2012), black carbon (also known as elemental carbon) refers to a solid form of mostly pure carbon produced by incomplete combustions that absorbs light (solar radiation) at all wavelengths. Measurements of this carbon species produced from light absorption measurements are referred to as BC, while those produced from thermal-optical methods are referred to as EC. Though these methods are meant to represent the same parameter, in practice the operational differences between methods and within the same method result in different concentration values being reported, even when measuring a fixed concentration and composition source (Yelverton et al., 2014).

Because the optical method is non-destructive and relatively low cost, it is of value to understand the relationship of the two measurements within the airshed being studied to evaluate the applicability of the optical BC measurement as a surrogate for elemental carbon. In Figure 2, BC concentrations are plotted vs EC concentrations for all sites and seasons combined. Measurements from the two techniques are well correlated, with $R = 0.9$, and their concentration values are similar, with a BC concentrations on average about 12% lower than EC concentrations. A summary of comparisons from numerous studies conducted since 2000 (U.S. EPA, 2012, Appendix 1) found the BC and EC measurement to have consistently high correlation (average $R = 0.86$) and BC/EC ratios ranging from 0.7 – 1.3 for 70% of the studies examined. Thus, comparisons are consistent with previously reported data and are reasonable in light of the differences between and within the measurement techniques. The optical method can be affected by the size and composition of the non-carbon particles on the sample filter, as well as by the mass absorption coefficient used to estimate BC mass concentration. The thermal-optical operationally defined and reported concentrations depend on the specific temperature profile used to separate the elemental and organic carbon fractions, and the method used to correct for artifact formation.

[Figure 2]

3.4. Meteorological Classifications

We developed meteorological classifications that synopsise wind direction and stability conditions prevalent during each 12-hour sampling period. The wind speed and direction component of the parameter was based on measurements made at the Radvanice site. The 1-hour average wind speed and direction values were matched to the corresponding 12-hour sampling periods, then classified as NE (315-135 degrees) or SW (135-315 degrees), with the assumption that the geography constrains the winds mostly along the SW-NE corridor, based on long-term data (see Figure S3 in the supporting material). The entire 12-hour period was classified as either NE or SW if at least eight of the 1-hour periods were classified consistently as being from one sector; otherwise it was identified as variable and not given a directional classification.

The stability component was based in part on temperatures measured at four permanent stations throughout the region located at successively higher altitudes to get a vertical temperature pseudo-gradient. The temperature gradient is combined with the wind speed measured at the Radvanice site to produce one of three stability parameters – good, bad, and other - with “bad” indicating the most stagnant conditions. The criterion for classification as good or bad was that the stability condition existed for at least 8 of the 12 sampling hours. Otherwise, the stability was classified as “other”. If both the direction and stability were variable, the condition was identified simply as “other”, with no directional designation.

The resulting meteorological classifications stratified by sampling season and time of day are summarized in Table 3. About one third of the spring sampling periods and one half of the fall sampling periods were identified as having SW winds. Two thirds of the sampling periods with SW winds were

identified as having variable (other) stability conditions, with most of the remaining having well-mixed (good) stability conditions. Slightly more than half of the sampling periods with NE winds were identified as having stagnant (bad) stability conditions, with the remaining having variable (other) stability conditions.

[Table 3]

3.5. Wind Direction Analyses

Samples were sorted by wind direction classification, site, and season. Average concentrations of particulate matter species were computed for each wind direction classification at each sampling site and season. 18% of spring samples and 12% of fall samples had no directional classification and were excluded from this analysis. The average concentration of the remaining NE and SW samples were computed, and the ratio of the average NE to SW concentrations (NE/SW) are compared graphically in Figure 3 for each sampling site and season.

[Figure 3]

Looking at Figure 3, one can see large differences in the NE/SW concentration ratio between the Radvanice site and the other two sites for species associated with the industrial complex, most notably Fe, Mn, and Cr. Because the Radvanice site is NE of the industrial complex, those species have higher concentrations at that site from the SW than from the NE, so the NE/SW ratio is well below 1. For example, the NE/SW ratio for Fe is 0.07 in the fall at the Radvanice site. The Radvanice site is also slightly elevated and may thus experience high plume impacts from the industrial complex. This is true in both seasons studied. At the Vratimov site, the opposite is true in both seasons studied because the industrial facility impacts that site when winds are from the NE. However, the directional disparity is

not as great for fine mass overall in either season, so there are sources other than the industrial complex that contribute to the total fine mass. In the fall, Figure 3 shows that the average fine mass concentration from the NE is greater than that from the SW at all sites. In the spring, the NE/SW ratio for fine mass concentration is 1.4 and 1.5 at Vratimov and Poruba, respectively, but close to 1 at the Radvanice site. This means that there is a source or sources to the NE contributing significantly to the fine mass concentration, even at the Radvanice site. The greater frequency of stagnant atmospheric conditions associated with the NE sector may also play a role in the concentration disparity. Sulfur followed a pattern similar to that of fine mass, though the directional disparity was not as strong as fine particle mass as a whole. The NE/SW ratio for sulfur ranged from 1.0 at Radvanice in the spring to 1.7 at Poruba in the fall.

Cl is the most strongly variable PM species between sites, seasons, and wind sectors, with the NE/SW ratio ranging from 0.14 (concentrations dominant for SW winds) at Radvanice in the spring to 8.8 (concentrations dominant for NE winds) at Vratimov in the fall. Further investigation of Cl should consider process emissions, particularly the sinter process, from the industrial complex, as well as salt/brine mixtures seasonally-applied to road surfaces.

EC (and BC) have higher concentrations from the NE than the SW in both seasons. The NE/SW ratios at Vratimov and Poruba are close to 2 in the spring and fall. At the Radvanice site, there is more of a SW component in the spring (NE/SW ratio 1.8 in fall, 1.2 in spring). OC also has higher concentrations from the NE than the SW in both seasons, with a slightly larger disparity in the fall (average NE/SW ratios range from 1.9 to 2.6) compared with the spring (average NE/SW ratios 1.6 at all sites). These results suggest a source or group of sources to the NE of the sampling sites contributing a greater fraction of the carbonaceous species overall, and that is more dominant in the fall than in the spring.

PAH concentrations are greater from the NE than the SW, especially for BaA (benzo(a)anthracene) and heavier PAH species, at all sites in the fall, and at Vratimov and Poruba in the spring. In the spring, the NE/SW heavy PAH ratio is greater at the Vratimov site than at the Poruba site, and close to 1 at the Radvanice site. It is interesting to look specifically at BaP (benzo(a)pyrene), both as a known carcinogen and as a PAH species representative of all heavy PAHs. In the fall, average NE/SW ratios were 1.8, 3.0, and 3.4 at Radvanice, Vratimov and Poruba, respectively. In the spring the average NE/SW ratios were, in the same site order, 1.1, 5.5, and 4.4. Based on these results, there appears to be a source of heavy PAHs to the SW of Radvanice (NE of Vratimov) that is just as prominent as the source NE of Radvanice. This shows the likely impact of the industrial complex, but also shows that the industrial complex is not the exclusive source of PAHs. It is likely that a source of these heavy PAHs to the NE of the Radvanice site is contributing substantially to the concentrations, and that source is more prominent in the fall than in the spring. A source meeting those criteria is home heating using cheap fuels such as wood and coal. It is possible that some of these likely home heating emissions are trans-border emissions.

4. Conclusions

The careful study design resulted in a set of data that is sufficient to reveal the likely source types driving the overall fine particulate matter pollution in the Ostrava metropolitan area of the Czech Republic. Seasonal comparisons were especially revealing. Overall, the results indicate a source or group of sources to the NE of all sampling sites that contributes significantly to the fine particle mass and PAH concentrations in the fall, and competes with contributions from the local industrial complex in the spring. A source meeting those criteria is home heating using inexpensive and high-emission fuels such as wood and coal. It is possible that some of these home heating emissions are trans-border emissions. The industrial source is still contributing to the local pollution, but it is not the exclusive source. There are regional and seasonal sources that are clearly making a big impact on the fine mass. It is not a situation of one source or the other – there are multiple sources and their relative impact depends on conditions and location. The data suggest that SO₂ is likely influenced by localized activities at the industrial complex as well as seasonal factors. The data presented here provide a qualitative overview of the results and form a solid foundation for the application of source apportionment models to be presented in a planned follow-on publication.

5. References

ATSDR (Agency for Toxic Substances and Disease Registry), 1995. Toxicological profile for Polycyclic Aromatic Hydrocarbons (PAHs). Atlanta, GA: U.S. Department of Health and Human Services, Public Health Service.

Černíkovský, L., Novák, J., Plachá, H., Krejčí, B., Nikolova, I., Chalupníčková, E., Conner, T., Norris, G., Kovalčík, K., Olson, D., Turlington, J., Croghan, C., Willis, R., Williams, R., 2013. The impact of select pollutant sources on air quality for Ostrava and the Moravian-Silesian metropolitan region by the Positive Matrix Factorization model, presented at the 2013 European Aerosol Conference, Prague, Czech Republic, 1-6 Sept., 2013.

Vossler, T., Černíkovský, L., Novák, J., Williams, R., 2014. Source apportionment of fine particulate matter in the Ostrava metropolitan region of the Czech Republic, 2014, in preparation.

Czech Statistical Office, 2013. <http://www.czso.cz/csu/2013edicniplan.nsf/engp/801011-13> , accessed September 2014.

European Commission, 2014. <http://ec.europa.eu/environment/air/quality/standards.htm>, accessed November 2014.

EEA (European Environment Agency), 2010. <http://www.eea.europa.eu/soer/countries/cz/air-pollution-why-care-czech-republic>, accessed September 2014.

EEA (European Environment Agency), 2014. European Union emission inventory report 1990–2012 under the UNECE Convention on Long-range Transboundary Air Pollution (LRTAP), Technical report No 12/2014. <http://www.eea.europa.eu/publications/lrtap-2014>, accessed September 2014.

European Parliament, Council of the European Union, 2008. Directive 2008/50/EC of the European Parliament and of the Council of 21 May 2008 on ambient air quality and cleaner air for Europe. Official Journal of the European Union L 152, Annex VI.

Hansen, A.D.A., 2005. The Aethelometer Manual, Magee Scientific, http://mageesci.com/images/stories/docs/Aethalometer_book_2005.07.03.pdf, accessed September 2014.

Kellogg, R.D., 2007. Spectral Analysis of Energy-Dispersive X-Ray Spectra of Ambient Aerosols, Alion Science and Technology, TR-WDE-07-02.

Ministry of the Environment of the Czech Republic, 2013. http://www.mzp.cz/en/air_protection, accessed September 2014.

Moldan, B., Schnoor, J.L., 1992, Czechoslovakia: Examining a critically ill environment, Environmental Science and Technology, Vol. 26, 14-21.

NIOSH (National Institute for Occupational Safety and Health), DHHS, 2003. P.F. O'Connor, P.C. Schlecht, Monitoring of Diesel Particulate Exhaust in the Workplace, Chapter Q, Third Supplement to NIOSH Manual of Analytical Methods (NMAM), 4th Edition, NIOSH, Cincinnati, OH. Publication No. 2003-154. <http://www.cdc.gov/niosh/docs/2003-154/pdfs/5040.pdf>, accessed September 2014.

Pinto, J.P., Stevens, R.K., Willis, R.D., Kellogg, R., Mamane, Y., Novak, J. Šantroch, J, Beneš, I. Leniček, J. Bureš, V., 1998. Czech Air Quality Monitoring and Receptor Modeling Study, *Environmental Science and Technology*, Vol. 32, 843-854.

Stevens, R.K., Pinto, J.P., Mamane, Y., Willis, R.D., 1996. Characterization and source apportionment of particulate matter in the Czech Republic. *Journal of Aerosol Science*, 27, S685-S686.

Turpin, B.J., Lim, H.J., 2001. Species Contributions to PM_{2.5} Mass Concentrations: Revisiting Common Assumptions for Estimating Organic Mass, *Aerosol Science and Technology*, 35:1, 602-610.

U.S. EPA (United States Environmental Protection Agency), 1981. 40 CFR, Part 423, Appendix A -126 Priority Pollutants.

U.S.EPA (United States Environmental Protection Agency) Report to Congress, 2012. Office of Air and Radiation, Office of Air Quality Planning and Standards. Research Triangle Park, NC. Report to Congress on Black Carbon: EPA-450/R-12-001. <http://www.epa.gov/blackcarbon/2012report/fullreport.pdf>, accessed September 2014.

Williams, R.W., Watts, R.R., Hartlage, T.A., Phillips, L., Lewtas, J., Dobias, L., Havrankova, J., Volf, J., Kellogg, R.B., Willis, R.D., Novak, J., 1997. Ostrava Human Exposure and Biomarker Study, EPA/600/R-97/069, August 1997.

Willis, R.D., Ellenson, W.D., Pinto, J.P., Hartlage, T.A., Novak, J., Dostalek, J., Černíkovský, L. Bureš, V., 1997. Ostrava Air Quality Monitoring and Receptor Modeling Study, EPA/600/R-97/030, April 1997.

Yelverton, T.L.B., Hays, M.D., Gullett, B.K., Linak, W.P., 2014. Black carbon measurements of flame-generated soot as determined by optical, thermal-optical, direct absorption, and laser incandescence methods, *Environmental Engineering Science*, Vol. 31, Number 4, 209-215.

Figure Captions

Figure 1. Map of Ostrava region and sampling locations: 1) Radvanice, 2) Vratimov, 3) Poruba.

Figure 2. Black carbon measured with optical method plotted vs. elemental carbon measured with thermal-optical method.

Figure 3. Ratios of the average NE/SW concentrations for spring and fall seasons.

Figure 1

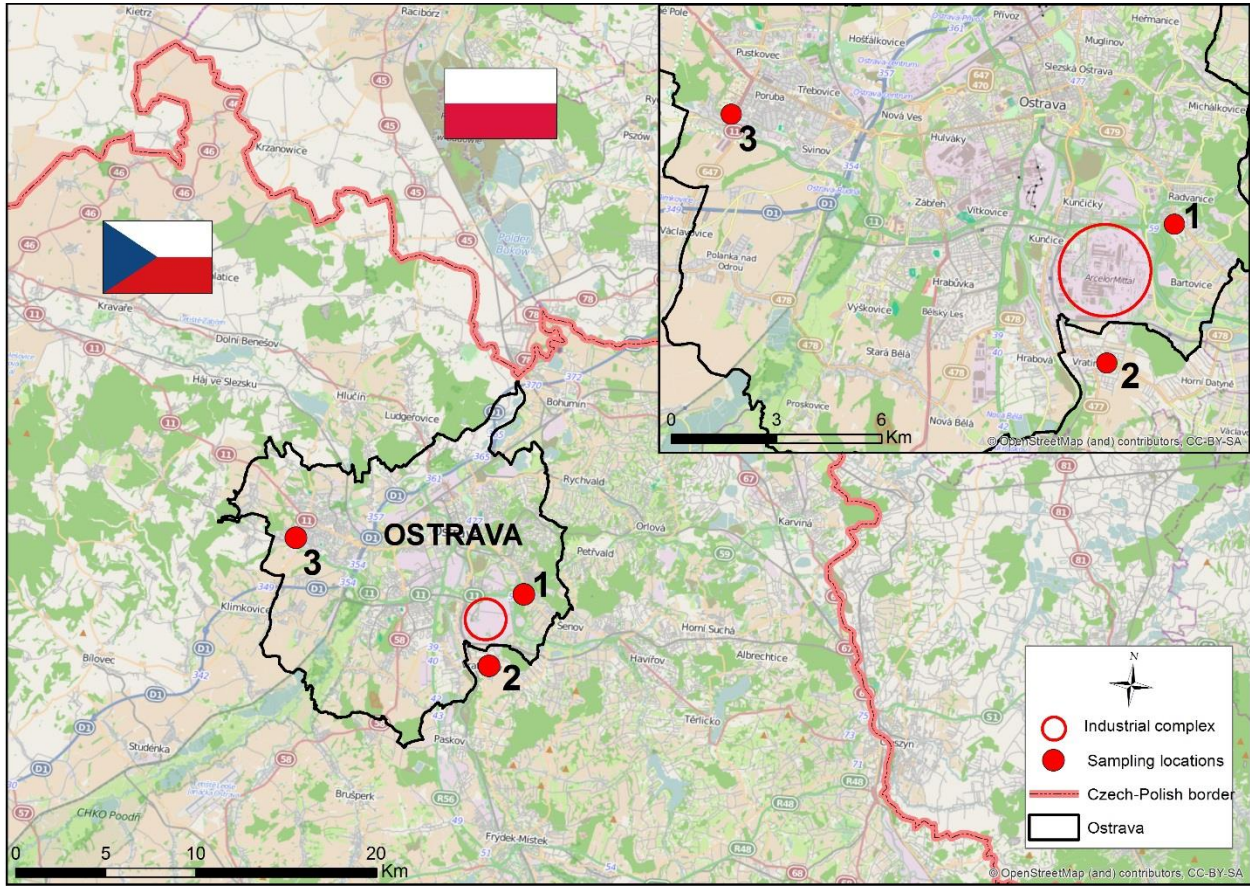


Figure 2

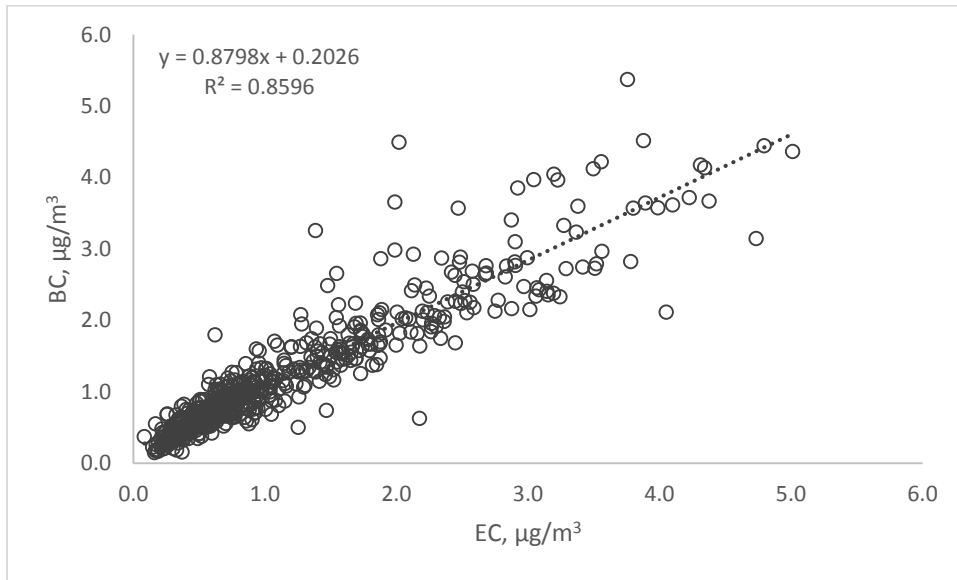


Figure 3

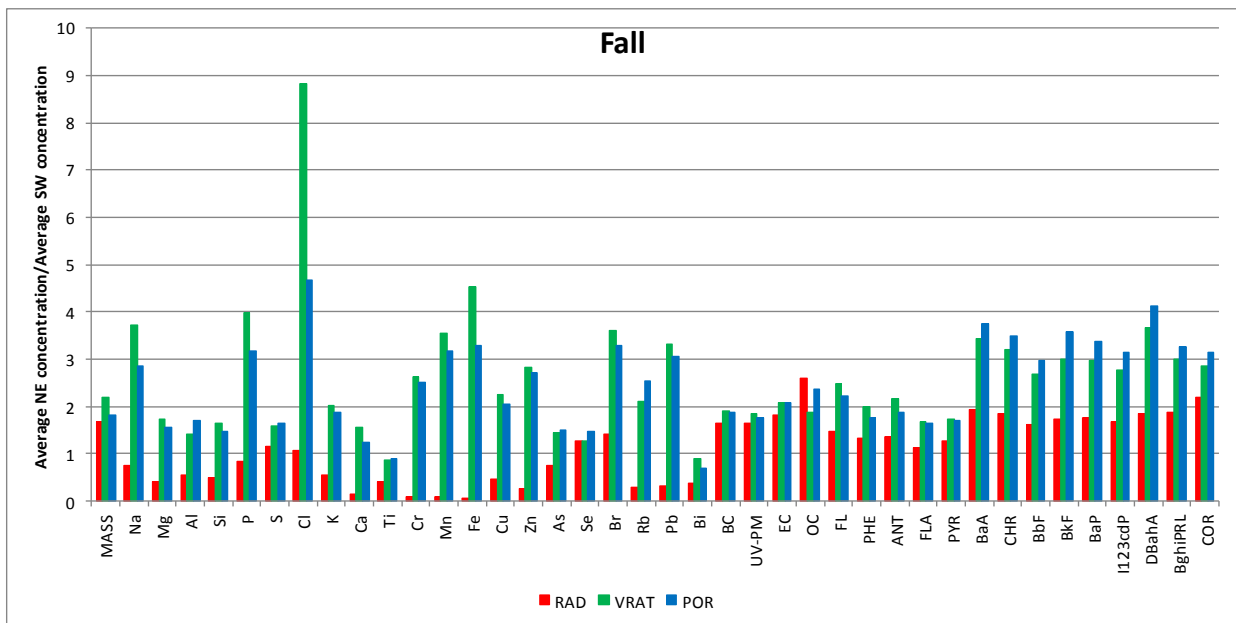
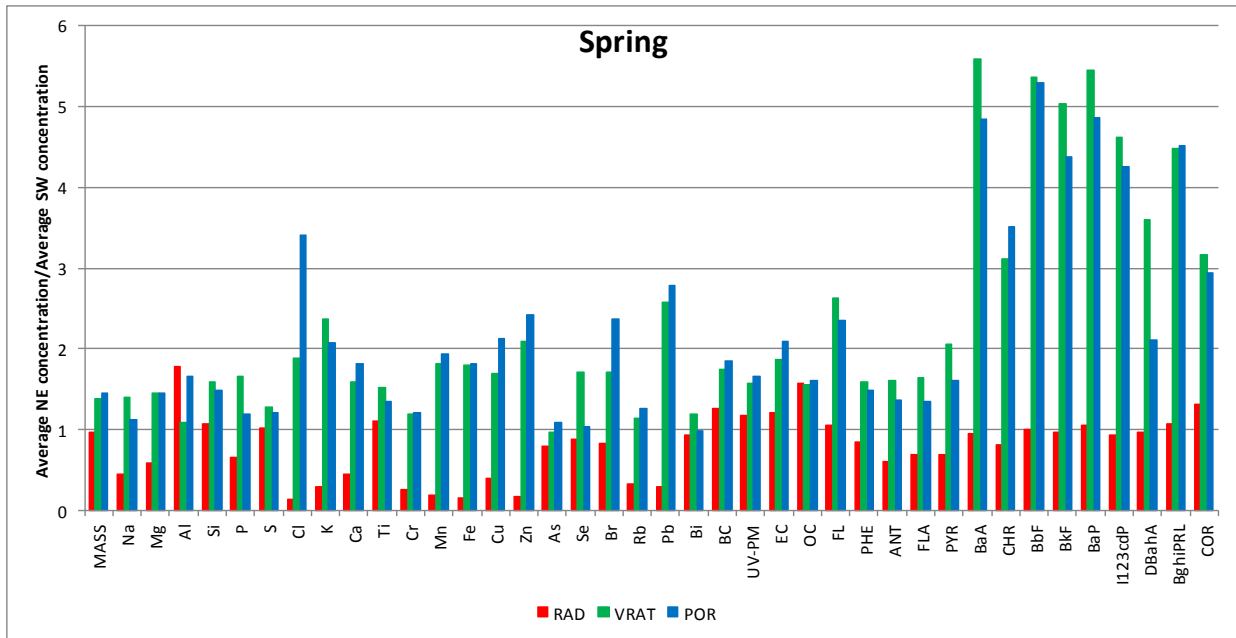


Table 1. Seasonal Stratifications of Selected Species: Average, Standard Deviation and Maximum Concentrations in ng/m³.

	Spring									Fall								
	Poruba (n=96) ^a			Vratimov (n=97)			Radvanice (n=97)			Poruba (n=98) ^b			Vratimov (n=99) ^c			Radvanice (n=99) ^d		
	Avg	Stds	Max	Avg	Stds	Max	Avg	Stds	Max	Avg	Stds	Max	Avg	Stds	Max	Avg	Stds	Max
PM _{2.5}	15 072	5 407	36 407	15 820	5 450	30 276	17 166	5 491	32 577	35 590	22 837	11 9527	40 019	26 198	117 866	49 083	25 716	130 530
Na	76	67	340	104	78	462	166	177	1 033	112	130	821	126	121	618	256	190	964
Mg	37	28	125	51	32	166	61	42	199	36	39	177	31	43	183	100	83	353
Al	65	98	579	87	102	617	61	119	650	44	71	324	41	73	347	62	124	374
Si	178	200	1 450	227	220	1 359	218	200	1 338	109	148	976	116	98	685	181	106	449
P	6	4	20	8	4	22	10	7	32	10	11	63	10	11	55	19	12	65
S	949	442	2 408	1 153	532	2 663	1 145	505	2 959	1 302	810	3 696	1 321	831	4 339	1 530	792	4 336
Cl	18	28	219	31	45	380	142	303	2 046	608	1 053	7 273	697	993	4 671	1 504	1 135	6 426
K	89	58	249	146	101	558	320	432	2 612	290	196	846	325	201	1 078	681	425	2 467
Ca	56	55	340	86	80	426	131	117	684	37	50	287	50	60	522	206	212	913
Ti	4	5	37	5	6	36	5	6	37	2	3	14	2	2	14	3	2	9
Cr	1	1	6	1	1	5	2	3	12	1	1	9	2	3	28	8	11	55
Mn	6	6	41	12	10	56	29	42	250	7	9	47	14	26	260	104	135	538
Fe	132	141	933	296	254	1 413	805	1 150	6 048	148	202	1 298	345	668	5 161	2 766	3 535	13 279
Cu	6	4	30	8	5	36	12	10	63	8	5	26	8	7	47	18	11	58
Zn	34	40	261	60	51	329	175	294	1 531	67	63	301	95	87	579	445	511	3 030
As	2	2	9	2	2	12	3	2	11	3	3	11	4	3	18	5	4	26
Se	2	1	5	2	1	6	2	1	6	2	2	6	2	1	6	2	2	6
Br	2	2	6	3	2	7	4	3	21	8	8	52	9	8	41	13	7	48
Rb	1	1	4	1	1	4	2	3	18	1	1	6	1	1	7	4	4	19
Pb	10	8	36	16	12	70	34	40	245	18	17	95	22	20	91	79	80	448
Bi	4	2	9	3	2	8	4	2	11	2	2	7	2	2	7	4	4	20
BC	585	257	1 181	656	261	1 396	745	252	1 551	1 494	879	4 446	1 692	930	5 375	2 069	919	4 517
UVPM	464	164	861	503	168	1 002	574	157	1 050	1 162	717	3 451	1 351	736	3 855	1 571	701	4 000
EC	544	292	1 523	526	259	1 444	680	264	1 520	1 649	1 051	4 797	1 615	991	4 378	1 889	988	5 013
OC	4 903	1 887	11 024	4 809	1 813	10 199	5 277	2 056	11 511	13 196	9 664	45 883	15 905	11 191	67 947	16 510	11 088	49 764
BaP	<1	<1	3	<1	2	12	2	3	14	6	6	28	7	6	26	12	6	31
ΣPAH	33	18	90	71	56	320	115	76	535	155	112	609	203	137	674	336	146	812

^aExcluded Poruba, 5/14/12, night, Cu = 143 ng/m³

^bExcluded Poruba, 10/24/12, day, Si = 5 199 ng/m³, Ca = 2 489 ng/m³, Ti = 38 ng/m³ (Coincided with nearby construction activities.)

^cExcluded Vratimov, 10/20/12, night, OC = 92 431 ng/m³; 10/25/12, day, Ti = 54 ng/m³; 10/26/12, day, OC = 70 027 ng/m³

^dExcluded Radvanice, 11/21/12, day, EC = 26 291 ng/m³, OC = 155 051 ng/m³, 12/6/12 day, Bi = 74 ng/m³

Table 2. – Diurnal Stratifications of Selected Species: Average, Standard Deviation and Maximum Concentrations in ng/m³.

	Day									Night								
	Poruba (n=97) ^a			Vratimov (n=97) ^b			Radvanice (n=96) ^c			Poruba (n=97) ^d			Vratimov (n=99) ^e			Radvanice (n=100)		
	Avg	Stds	Max	Avg	Stds	Max	Avg	Stds	Max	Avg	Stds	Max	Avg	Stds	Max	Avg	Stds	Max
PM _{2.5}	23 116	17 432	119 527	28 000	22 306	17 866	31 226	21 679	126 216	27 443	21 148	117 303	28 314	23 311	110 950	35 266	26 999	130 530
Na	104	106	709	125	109	593	242	221	1 033	83	103	821	105	96	618	182	146	667
Mg	40	34	177	45	39	166	87	68	353	32	32	144	37	40	183	74	69	314
Al	63	91	579	80	101	617	100	111	650	46	80	434	48	79	517	26	120	401
Si	191	218	1 450	214	200	1 359	251	178	1 338	95	113	780	130	144	1 063	150	123	884
P	8	8	48	9	9	55	16	11	56	7	9	63	8	8	50	13	11	54
S	1 171	708	3 696	1 307	764	4 339	1 411	764	4 004	1 080	640	3 365	1 159	630	3 449	1 272	609	4 336
Cl	261	657	4 480	338	700	3 974	774	1 009	4 668	364	930	7 273	404	872	4 671	884	1 140	6 426
K	176	152	830	251	189	1 078	543	535	2 612	201	194	846	223	179	851	463	383	1 720
Ca	64	65	340	86	82	522	199	178	941	29	29	212	50	58	426	140	169	871
Ti	4	5	37	5	5	36	5	5	37	2	3	17	3	3	26	3	3	25
Cr	1	1	7	2	3	28	5	9	55	1	1	9	1	1	9	5	8	43
Mn	7	9	47	14	25	230	68	105	538	5	6	38	12	14	81	65	109	480
Fe	175	207	1 298	363	593	5 161	1 852	2 778	13 279	102	120	997	283	418	2 326	1 742	2 854	12 857
Cu	7	5	30	8	6	47	16	11	63	6	4	23	8	5	36	14	11	58
Zn	52	53	288	81	79	579	296	371	1 692	49	57	301	75	69	446	327	496	3 030
As	3	2	10	3	3	18	4	4	26	3	3	11	3	3	12	4	3	13
Se	2	1	5	2	1	6	2	1	6	2	1	6	2	1	6	2	1	6
Br	5	6	40	6	5	33	8	6	39	5	7	52	6	7	41	9	8	48
Rb	1	1	6	2	1	7	4	4	19	1	1	5	1	1	5	3	3	13
Pb	14	13	73	18	17	91	57	69	448	14	14	95	20	17	82	56	66	311
Bi	3	2	8	3	2	7	3	3	18	3	2	9	3	2	8	4	4	20
BC	970	696	3 721	1 172	822	4 220	1 340	878	4 138	1 109	880	4 406	1 197	915	5 375	1 484	1 007	4 517
UVPM	739	481	2 622	917	626	3 138	988	584	2 532	893	741	3 451	945	738	3 855	1 163	813	4 000
EC	1 036	863	4 226	1 093	889	4 099	1 281	924	4 344	1 147	1 033	4 797	1 047	930	4 378	1 299	968	5 013
OC	7 955	6 573	44 961	10 718	10 613	67 947	9 964	8 510	45 355	10 119	9 346	45 883	9 995	8 907	40 847	11 898	10 812	49 764
BaP	2	4	17	4	5	17	6	6	20	4	6	28	4	6	27	8	7	31
ΣPAH	81	81	394	134	114	474	202	143	649	106	116	609	143	134	674	250	174	812

^aExcluded Poruba, 10/24/12, day, Si = 5 199 ng/m³, Ca = 2 489 ng/m³, Ti = 38 ng/m³ (Coincided with nearby construction activities.)

^bExcluded Vratimov, 10/25/12, day, Ti = 54 ng/m³; 10/26/12, day, OC = 70 027 ng/m³

^cExcluded Radvanice, 11/21/12, day, EC = 26 291 ng/m³, OC = 155 051 ng/m³, 12/6/12 day, Bi = 74 ng/m³

^dExcluded Poruba, 5/14/12, night, Cu = 143 ng/m³

^eExcluded Vratimov, 10/20/12, night, OC = 92 431 ng/m³;

Table 3. Meteorological Classifications – seasonal and diurnal.

	SPRING DAY	SPRING NIGHT	FALL DAY	FALL NIGHT
SW-GOOD	7	1	3	5
SW-OTHER	16	9	26	14
SW-BAD	0	0	1	2
NE-GOOD	0	0	0	0
NE-OTHER	16	10	8	4
NE-BAD	0	21	3	22
OTHER	9	8	8	4

Supporting Material:

An investigation of local and regional sources of fine particulate matter in the Ostrava metropolitan region of the Czech Republic

T. Vossler¹, L. Černíkovský², J. Novák², H. Plachá², B. Krejčí², I. Nikolova², E. Chalupníčková², R. Williams¹

¹U.S. Environmental Protection Agency, Office of Research and Development, Research Triangle Park, North Carolina, USA

²Czech Hydrometeorological Institute, Prague, Czech Republic

Table of Contents

Figure S1 - Wind rose, Ostrava-Mošnov, 2004-2013

Table S1 – Measurement and monitoring equipment and methods

Text S1 – Calculation of black carbon concentrations and uncertainty

Text S2 – Teflon filter deposit areas and uncertainty estimates

Text S3 – GC-MS analytical details

Text S4 – Uncertainty estimates for measured and replacement PAH concentrations

Figure S2 – Time series plots of selected metals and non-metals at Radvanice site

Tables S2a and S2b - Correlation coefficients of gases, Radvanice site, spring (a) and fall (b).

Figure S3 – 12-hour SO₂ time series plots

Figure S1. Wind rose, Ostrava-Mošnov, 2004-2013

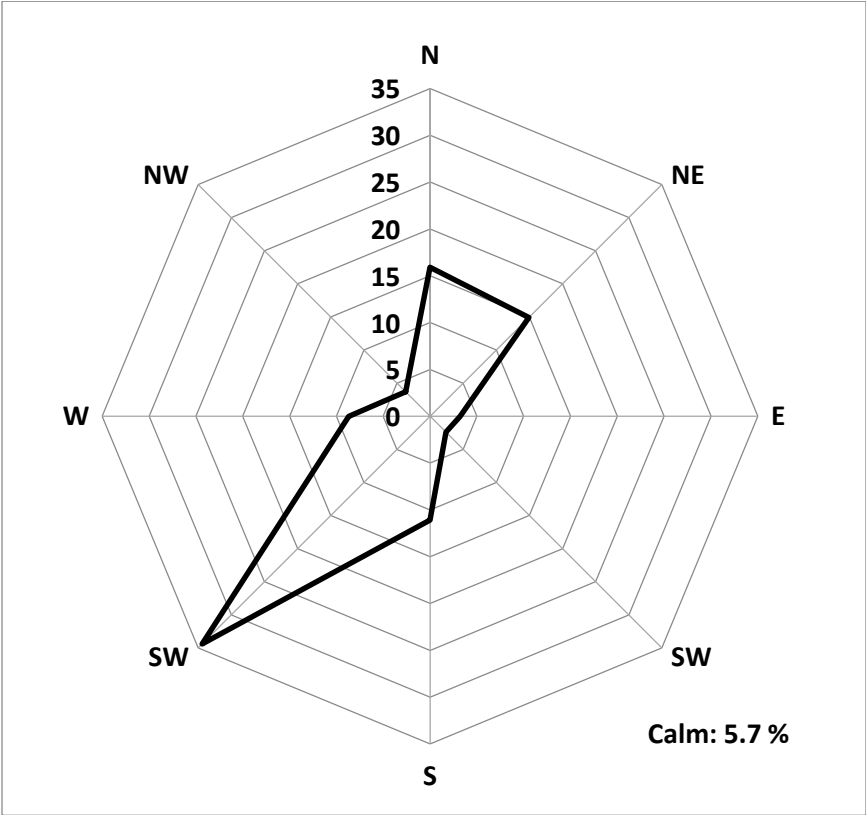


Table S1. Measurement and monitoring equipment and methods.

Parameter Measured	Analytical/Measurement Method	Instrument Type/Model (Company Name/Location)	Averaging Time	Location ^a
PM _{2.5} mass elements black carbon	gravimetry EDXRF transmissometry	MX5 microbalance (Mettler Toledo, Greifensee Switzerland) Epsilon5 EDXRF (PANalytical, Almelo, The Netherlands) OT-21 dual wavelength transmissometer (Magee Scientific, Berkeley, CA, USA)	12-hr	P, V, R
elemental and organic carbon	thermal-optical	Sunset Laboratory (Tigard, OR, USA)	12-hr	P, V, R
PAHs	GC-MS	Agilent 7890A GC with series MSD (Agilent, Usti nad Labem, Czech Republic)	12-hr	P, V, R
PM10	radiometry	Thermo ESM Andersen FH 62 I-R (ESM Andersen Instruments GmbH, Erlangen, Germany)	10-min, 1-hr	V, R
SO ₂	ultraviolet fluorescence	TEI model M43 (Thermo Environmental Instruments, Franklin, MA, USA)	10-min, 1-hr	P, V, R
NO _x , NO ₂ , NO	chemiluminescence	TEI model M42 (Thermo Environmental Instruments, Franklin, MA, USA)	10-min, 1-hr	V, R
CO	infrared correlation absorption spectrometry	TEI model M48 (Thermo Environmental Instruments, Franklin, MA, USA)	10-min, 1-hr	V, R
O ₃	ultraviolet absorption photometry	TEI model M49 (Thermo Environmental Instruments, Franklin, MA, USA)	10-min, 1-hr	V, R
benzene, toluene	gas chromatography – photoionization detection	VOC71M gas analyzer (Environment S.A, Poissy Cedex, France)	1-hr	V, R
wind direction and velocity	ultrasonic anemometer	WindSonic (Gill Instruments Ltd, Lymington, Hampshire, UK)	10-min, 1-hr	V, R
global radiation	temperature difference method	SG 420 (TM, Tlustak, Praha, Czech Republic)	10-min, 1-hr	V, R
relative humidity	capacitance sensor	NH 421 (Comet System, Roznov pod Radhostem, Czech Republic)	10-min, 1-hr	V, R
air temperature	resistance method	NH 421 (Comet System, Roznov pod Radhostem, Czech Republic)	10-min, 1-hr	V, R

^aP = Poruba, V = Vratimov, R = Radvanice

Text S1. Calculation of black carbon concentrations and uncertainty estimates

Black carbon (BC) was measured by ORD using a light transmission method in which concentration measurements are made by comparing light absorbed at a given wavelength by the sample filter with light absorbed by a blank reference filter. The instrument used in this study operates at two different wavelengths: BC is measured with the infrared (880nm) source, while a parameter referred to simply as UV-PM is measured with the ultraviolet (370 nm) source. The latter is thought to represent mainly aromatic organic species. While not the primary focus of this analysis, it was included for completeness.

The measurement itself is simple, though the method for arriving at a volumetric concentration for the measurement is more involved. The instrument reports measurements in attenuation units, $ATN = 100 \times \ln(I_0/I)$, where I_0 = light transmitted through blank filter, I = light transmitted through loaded filter, and $100 =$ conversion of g/m^2 units to $\mu g/cm^2$ units (i.e., $1 g/m^2 = 10^6 \mu g/10^4 cm^2$).

The black carbon (BC) area concentration in $\mu g/cm^2$ is proportional to light attenuation (ATN) via BC ($\mu g/cm^2 = ATN/\sigma$, where σ (m^2/g) = mass attenuation coefficient. The value of mass attenuation coefficient depends on sample composition, wavelength, collection substrate, and other factors. Values reported in the literature for the attenuation coefficient vary widely and depend on the nature of the samples and the measurements methods and conditions. Attenuation coefficient values recommended by the instrument manufacturer - $16.6 m^2/g$ for BC and $39.5 m^2/g$ for UV-PM - were applied to these measurements.

To get the volume concentration in $\mu g/m^3$, the area (cm^2) of the sample deposit in cm^2 was multiplied the area concentration ($\mu g/cm^2$, computed as explained above). The resulting value (μg) was divided by the sample volume (m^3). The area was determined as described in a previous section of this document.

Volumetric concentration uncertainties include uncertainties of the measurement itself, as well as uncertainties from the area and volume estimates. As for PAH measurement uncertainties, the BC uncertainties were computed as $\sqrt{(EF \times \text{conc})^2 + (0.5 \times DL)^2}$. The DL (detection limit) was based on 3 times the standard deviation of the averaged field blank measurements (fall and spring combined). The EF (error fraction) was assumed to be 10%, the area uncertainty was based on the approach described previously to arrive at an average area ($10.9 \pm 0.9 \text{ cm}^2$), and the volume uncertainty was assumed to be 5%. All sources of uncertainty were propagated to compute the volumetric concentration uncertainties. No uncertainty was assigned to the mass attenuation coefficient.

Text S2. Teflon filter deposit areas and uncertainty estimates

The XRF and BC analyses yield concentrations in units of mass per deposit area. These area concentrations needed to be converted to volume concentrations for application in source apportionment models. This conversion depends on reliable information on the sampling conditions (flow rate, volume), the sample deposit areas, and realistic uncertainties of each of these parameters.

Deposit areas are typically well defined and can be determined with a high degree of precision and accuracy, but that is not the case with these filters. Some of the filters have full, uniform coverage (e.g., Poruba filters, with a few exceptions), but most have asymmetrical coverage or somewhere in between (e.g., mostly symmetrical but with thinner deposit at edges). CHMI determined that particle losses were unlikely, so further area evaluations were conducted with that assumption.

Collocated symmetrical and asymmetrical deposit filters collected at the Radvanice site were used to evaluate whether using different sample areas is appropriate for the two types of deposits. The evaluation revealed that there is insufficient information to recommend different deposit areas for filters with symmetrical vs. asymmetrical deposits. Thus, a single filter deposit area with relatively high uncertainty was selected to apply to all filter data.

The average asymmetrical diameter was estimated to be $10.2 \pm 0.8 \text{ cm}^2$ and the average symmetrical diameter was estimated to be $11.6 \pm 0.3 \text{ cm}^2$. Averaging these areas and propagating their uncertainties yields an area of $10.9 \pm 0.9 \text{ cm}^2$. This averaged deposit area and uncertainty was applied to both XRF and BC filter data.

Text S3. GC-MS analytical details

CHMI analyzed PM_{2.5} quartz filter (diameter of 47 mm) and PUF (50x100 mm) samples for 14 polynuclear aromatic hydrocarbon (PAH) compound via gas chromatograph-mass spectrometry, i.e., GS-MS (Agilent 7890A GC with 5975 series MSD, Usti nad Labem, Czech Republic). Quartz filters were extracted with dichloromethane using soxhlet extraction apparatus Buchi B-811. PUF were extracted with hexane using soxhlet extraction apparatus Buchi B-811 LVS (larger sample volume configuration). Both PUF and quartz filter extracts were combined and concentrated under a nitrogen stream (Zymark Turbovap II) down to a volume of 1 ml and then purified by column chromatography with silica gel. PAH fractions were concentrated under a nitrogen stream (Zymark Turbovap II) down to a volume of 500 µl and adjusted to 1 ml with hexane. Samples were analyzed by gas chromatography with mass spectrometric detection (GC/MS). PAHs separation was performed on DB-5 column (30 m x 0.25 mm x 0.25 µm). For quantification of PAHs was used internal standard method.

Text S4. Uncertainty estimates for measured and replacement PAH concentrations

In the PAH data set provided by CHMI, some concentrations were reported as <QL (quantifiable limit).

The PMF model requires either a numerical value or a missing value. The simplest solution is to substitute all concentrations reported as below a certain threshold with a replacement value. These are typically some fraction of the detection limit; e.g., $(1/\sqrt{2}) \times DL$. For the PAH data, we took a similar approach and substituted all concentrations reported as <QL with $(1/\sqrt{2}) \times QL$.

The PMF model also requires a numerical value for the uncertainty. Following PMF model guidance, the uncertainty for concentration greater than the DL was computed as $\sqrt{(EF \times conc)^2 + (0.5 \times DL)^2}$, where EF is the error fraction (also known as the coefficient of variation) for the method. For concentrations well above DL, this simplifies to $EF \times conc$, and increases in value as the concentration approaches the reported DL. For the latter, the replacement uncertainty for the replacement concentration was set equal to $2 \times EF \times conc$. While this approach does not precisely follow the typical uncertainty estimate, it is sufficient for these purposes, since PMF requires nothing more than a reasonable estimate. Any details of the specific uncertainty values are lost since all such values can be up-weighted within the model to diminish the influence of less certain data on the model results.

Figure S2. Time series plots of selected metals and non-metals at Radvanice site

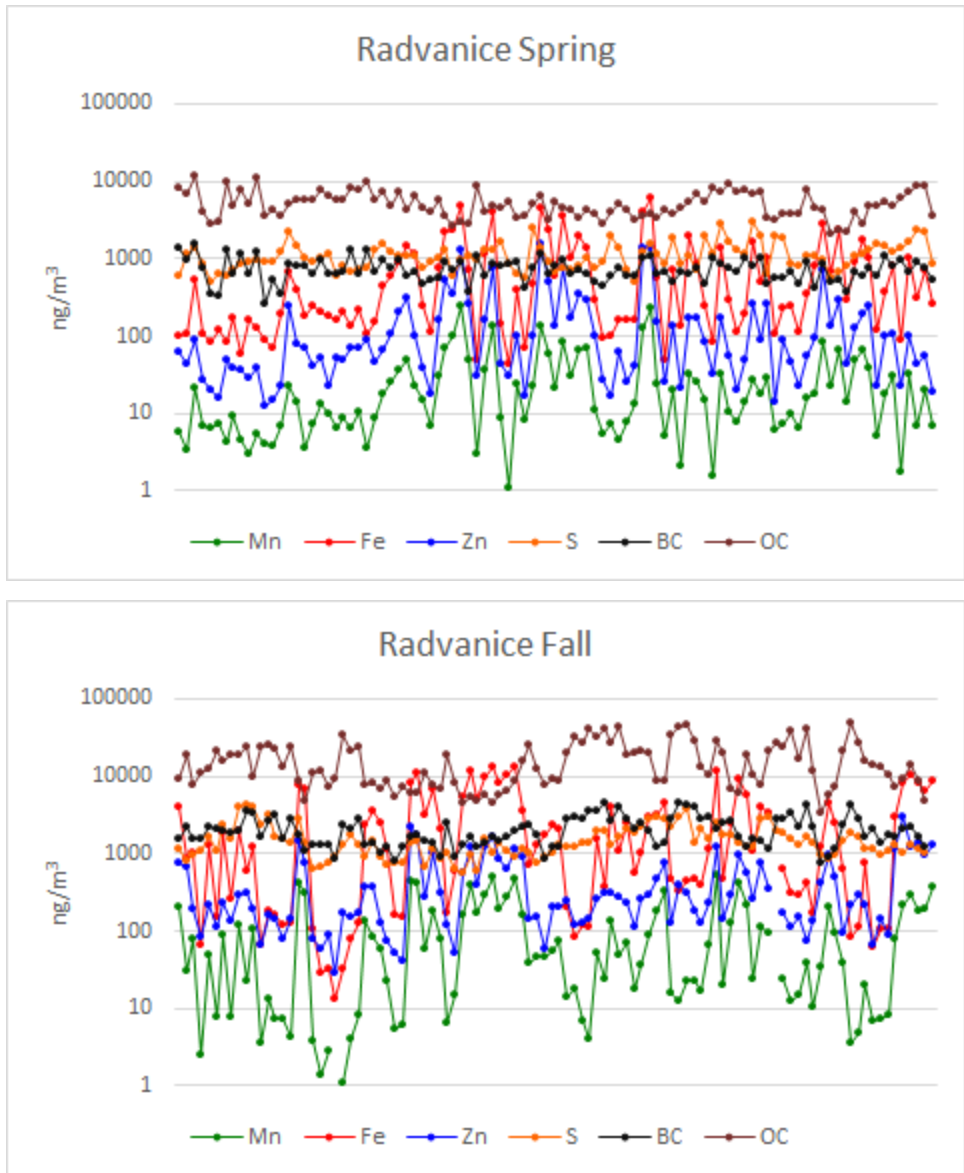


Table S2a. Correlation coefficients of gases, Radvanice site, spring.

	SO ₂	NO ₂	NO _x	PM10	BZN
SO ₂	1				
NO ₂	0.48	1			
NO _x	0.51	0.97	1		
PM10	0.46	0.63	0.58	1	
BZN	0.10	0.33	0.33	0.27	1

Table S2b. Correlation coefficients of gases, Radvanice site, fall.

	SO ₂	CO	NO ₂	NO _x	PM10	BZN
SO ₂	1					
CO	0.67	1				
NO ₂	0.31	0.60	1			
NO _x	0.21	0.58	0.86	1		
PM10	0.29	0.62	0.69	0.65	1	
BZN	-0.20	0.24	0.47	0.52	0.63	1

Figure S3. 12-hour average SO₂ time series plots.

